

EGU2020-8952:
**Revealing of surface deformations induced by geodynamic
processes in the Kuril island arc from GNSS data**

Yury Gabsatarov^{1,2}, Irina Vladimirova^{1,2}, Grigory Steblov^{2,4}, Leopold Lobkovsky^{1,3}
and Ksenia Muravieva¹

1 - *Moscow Institute of Physics and Technology, Moscow, Russia*

2 - *Geophysical Survey RAS, Obninsk, Russia*

3 - *Shirshov Institute of Oceanology RAS, Moscow, Russia*

4 - *Schmidt Institute of Physics of the Earth RAS, Moscow, Russia*

Our motivation:

Kuril subduction zone is one of the most active continental margins due to the high plate convergence rate. The 2006-2007 Simushir earthquakes with $M > 8$ started a new episode in the seismic history of this region. Correct geodetic characterization of surface deformations recorded prior, at time and after the 2006-2007 Simushir earthquakes is necessary for studies of regional geodynamical processes associated with seismic cycles and the evolution of the subduction zone.

Our goals:

- We want to develop an algorithm for processing observational data in Kuril region that would allow us to obtain correct estimates of the displacements caused by various geodynamic processes.
- We want to find out whether the GNSS data provides an evidence of the fault-block structure of the continental margin, proposed earlier on the basis of seismological and geological data.

In 2006-2008 Kuril GNSS network was installed along the island arc to provide information on the dynamics of the continental margin (Fig. 1). The GNSS stations located on the flanks of the Kuril arc were deployed before the 2006-2007 Simushir earthquakes (with $M > 8$), while GNSS stations near the source were deployed only 0.5-2 years after.

Since Kuril network has some disadvantages such as small amount of continuous stations (cGNSS), large gaps in observational data and near-linear arrangement stations, special attention must be paid to correct processing of the GNSS data to exclude miscalculations that can affect further modeling of regional geodynamical processes.

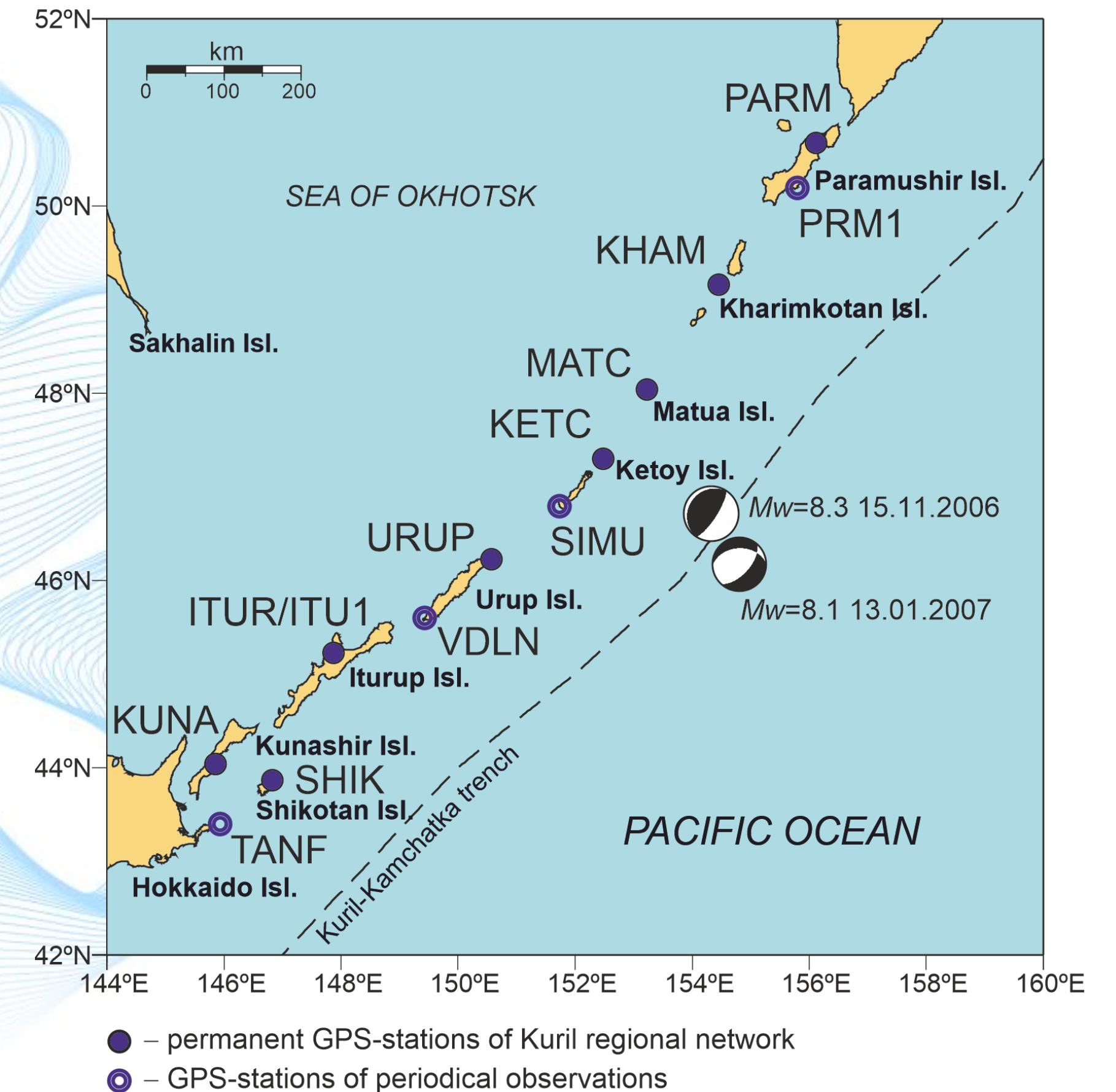


Fig.1 Final configuration of Kuril geodetic network

Initial processing of the KurilNet GPS observations was performed using the GAMIT/GLOBK software [Herring et al. 2018a; Herring et al. 2018b] in a three-steps manner described in [Kogan et al. 2013]. The result of processing was more than 9 years long time series of daily positions of KurilNet stations in the ITRF2008 reference frame relative to NAM (Fig. 2).

One of the main difficulties in processing of KurilNet data is that some of the GNSS stations were deployed only after large 2006-2007 Simushir earthquakes and their time series were dominated by intense and long-term postseismic transient processes such as afterslip and viscoelastic relaxation in the upper mantle.

These postseismic processes act almost simultaneously, which requires us to apply a special technique to distinguish their effects in recorded time series of spatially distributed GNSS stations.

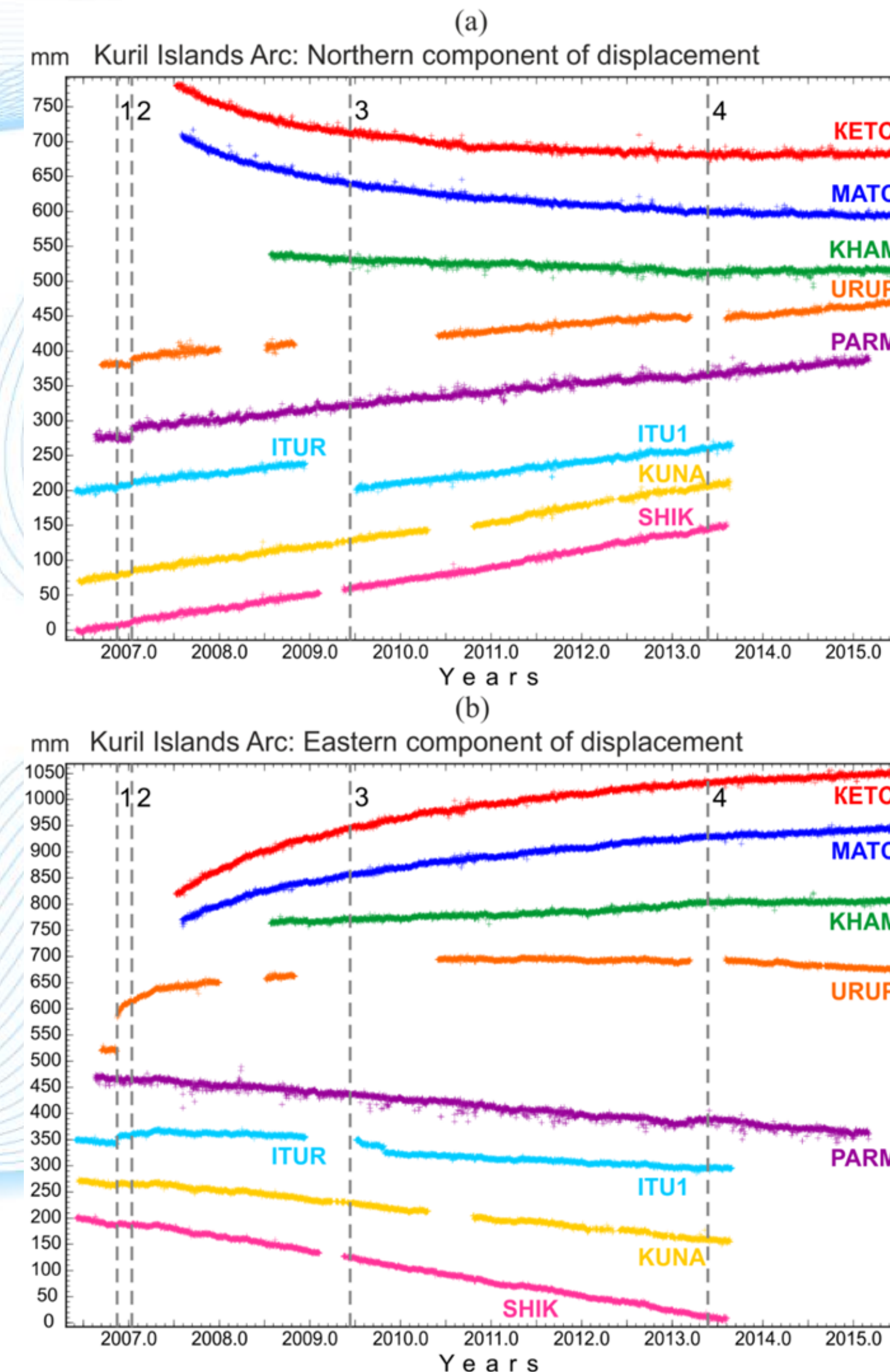


Fig.2 Timeseries of KurilNet stations. Moments indicated by dashed lines:
1 – 2006 Simushir earthquake,
2 – 2007 Simushir earthquake,
3 – 2009 Sarychev's peak eruption on Matua island,
4 – 2013 deep-focus Okhotsk earthquake

KurilNet stations, even the closest to the source of the 2006 Simushir, earthquake are located in the far-field zone, thus viscoelastic relaxation effects predominate in their time series from more than six months after the earthquake [Kogan et al., 2013]. We use this assumption to separate effects of afterslip and viscoelastic relaxation in the time series.

Our approach to the processing of the data of the KurilNet stations involves preliminary subtraction of the direct model of the viscoelastic relaxation in the asthenosphere following the 2006 Simushir earthquakes [Vladimirova et al., 2020] and further regression analysis of residual time series.

The viscoelastic relaxation model was obtained using VISCO1D software [Pollitz et al., 1997] on the basis of the three-year time series of displacements recorded after the 2006 Simushir earthquake on four nearest to the source GNSS stations (Fig. 3).

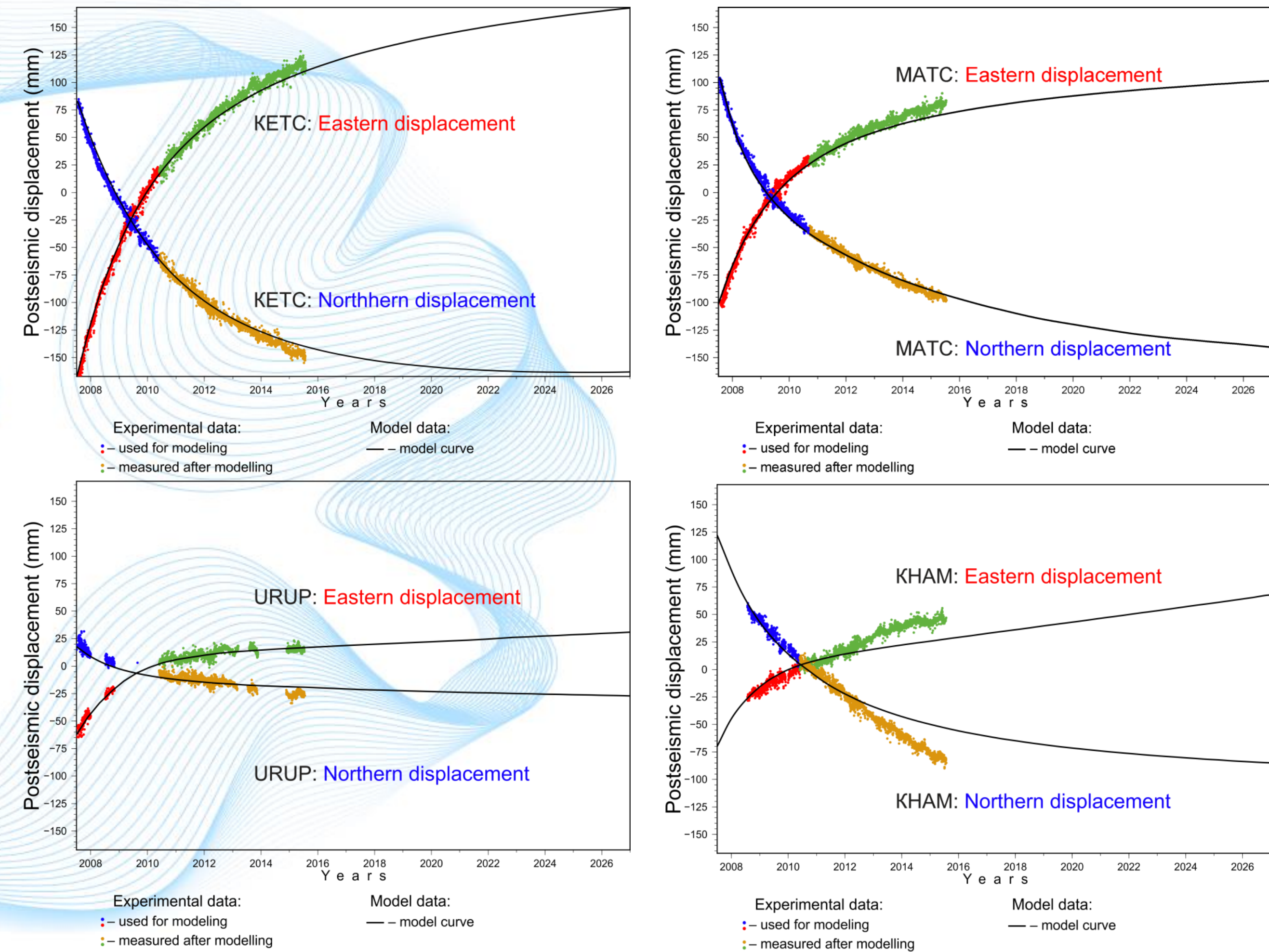


Fig.3 The model of viscoelastic relaxation for GNSS stations nearest to the source of the 2006 Simushir earthquake.

We construct a station motion model using the widely used regression analysis approach:

$$y(t_i) = a + bt_i + c\sin(2\pi t_i) + d\cos(2\pi t_i) + e\sin(4\pi t_i) + f\cos(4\pi t_i) + \\ + \sum_{j=1}^{n_g} g_j H(t_i - T_g^j) + \sum_{j=1}^{n_h} h_j H(t_i - T_h^j) + \sum_{j=1}^{n_k} k_j H(t_i - T_k^j) H(T_k^{j+1} - t_i) t_i + \\ + \sum_{j=1}^{n_l} l_j \ln(1 + (t_i - T_l^j)/m_j) H(t_i - T_l^j) + \sum_{j=1}^{n_p} p_j \exp(-(t_i - T_p^j)/r_j) H(t_i - T_p^j) + \varepsilon_i$$

As a result our model allows us to distinguish components which are related to: 1) long-term accumulation of elastic stresses, 2) almost instant release of substantial part of accumulated stresses during main shock (coseismic offsets), 3) transient processes following large earthquakes, 4) seasonal variations.

The main advantages of the proposed regression analysis algorithm are: 1) an automated process for detecting coseismic displacements, based on direct modeling of surface deformations using a dislocation model, 2) an automated process for identifying transient processes, 3) taking into account the realistic GNSS noise model in calculating errors.

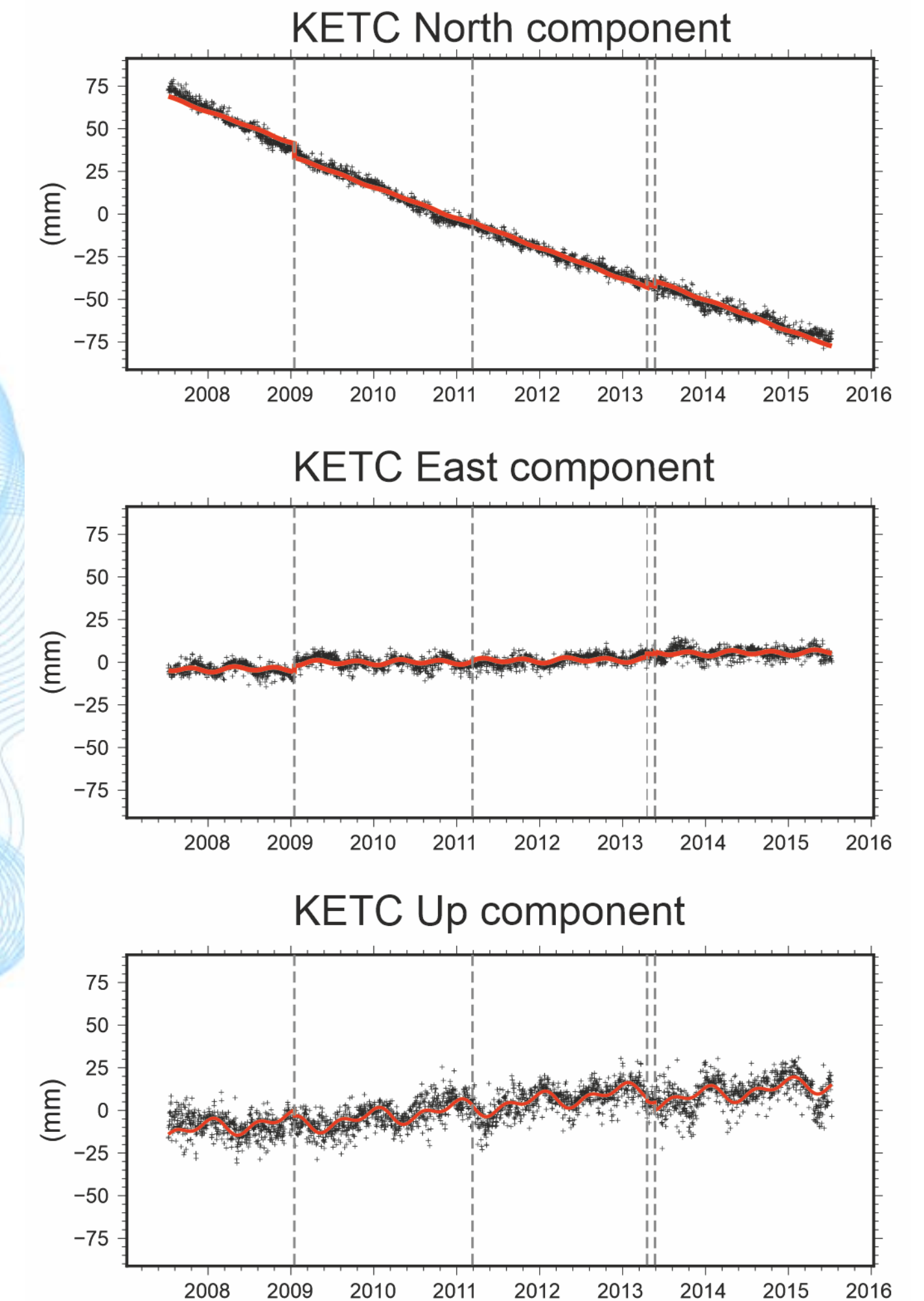


Fig. 4 An example of a regression model for KETC station (Ketoy island, Kurils)

The construction of a GNSS station motion model is carried out on the basis of the iterative scheme (Fig. 5), which includes the following main stages: 1) stage of data preparation and cleaning; 2) stage of modeling of nonlinear postseismic effects; 3) stage of constructing a complete covariance matrix of errors and the resulting regression model.

At stage I, the time series is cleaned of outliers, and the moments of earthquakes are determined based on an automated algorithm involving the direct calculation of coseismic deformation fields using GCMT data [Ekström et al., 2012].

At stage II the magnitudes and the attenuation constants of nonlinear postseismic effects are estimated. The attenuation constants are determined by iterating through predetermined values under the condition of minimizing the chi-square statistics.

At stage III, a complete model is built taking into account the seasonal signal represented by harmonic oscillations with a period of 1 year and 0.5 year. At this stage, the construction of the total GNSS noise, which is considered as a combination of white and flicker noise, also takes place [Williams et al., 2003].

At each stage of the iterative scheme, a statistical significance check is performed using the standard F-test.

The constructed seasonal signal model is checked by analyzing the amplitude spectrum of a GNSS signal using a non-equidistant discrete Fourier transform.

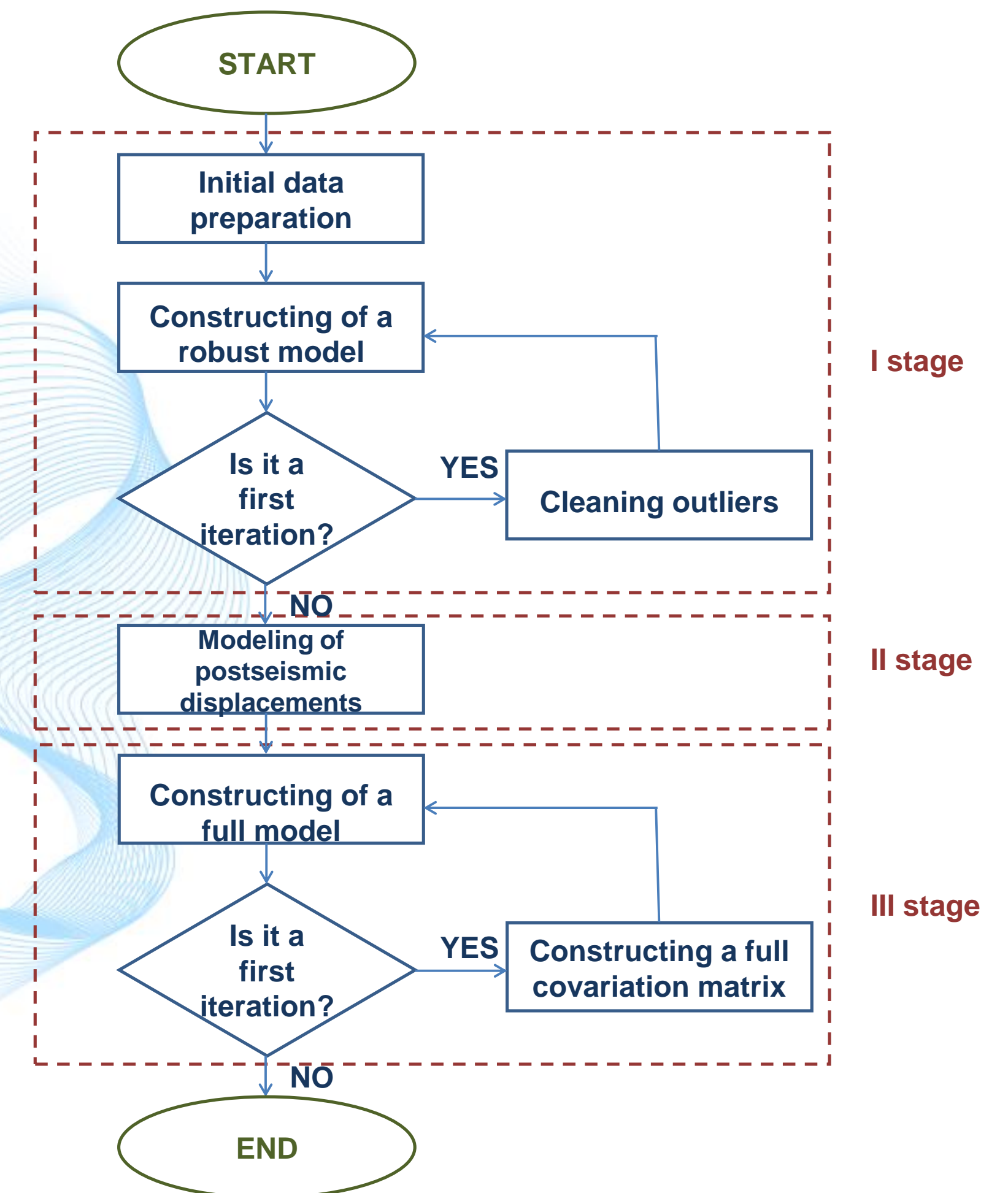


Fig.5 Iterative scheme of regression analysis

Constructed regression models for KurilNet stations allow us to analyze time series representing only slow aseismic motion (without seasonal variations and instant shifts).

Earlier a hypothesis of the fault-block structure of the central part of the Kuril island arc was proposed on the basis of seismological data and data obtained during the complex oceanographic expeditions carried out in this region in 2005–2006 [Baranov et al., 2015]. According to these data the central part of the Kuril island arc is divided into 10 blocks with the characteristic sizes from 30 to 100 km (Fig. 6).

We calculated annual variations of velocities of station motions (Fig. 7) that provide clear evidence of abrupt changes in directions and rates of station consistent with the block-like motion hypothesis.

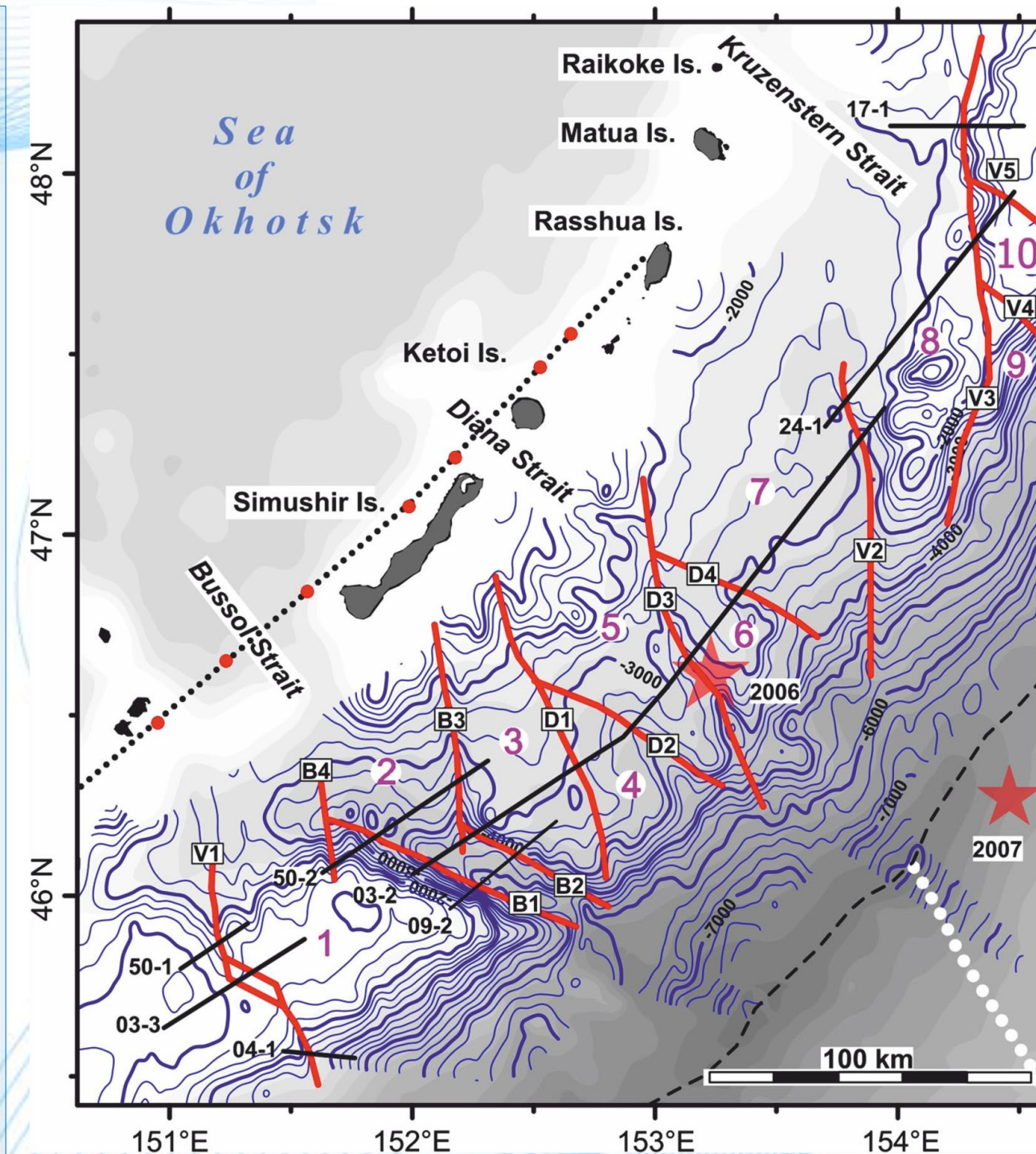


Fig.6 Location of the main identified transcurrent faults (red solid lines) in the Central Kuril Islands forearc region based on the data of geophysical surveys [Baranov et al., 2015].

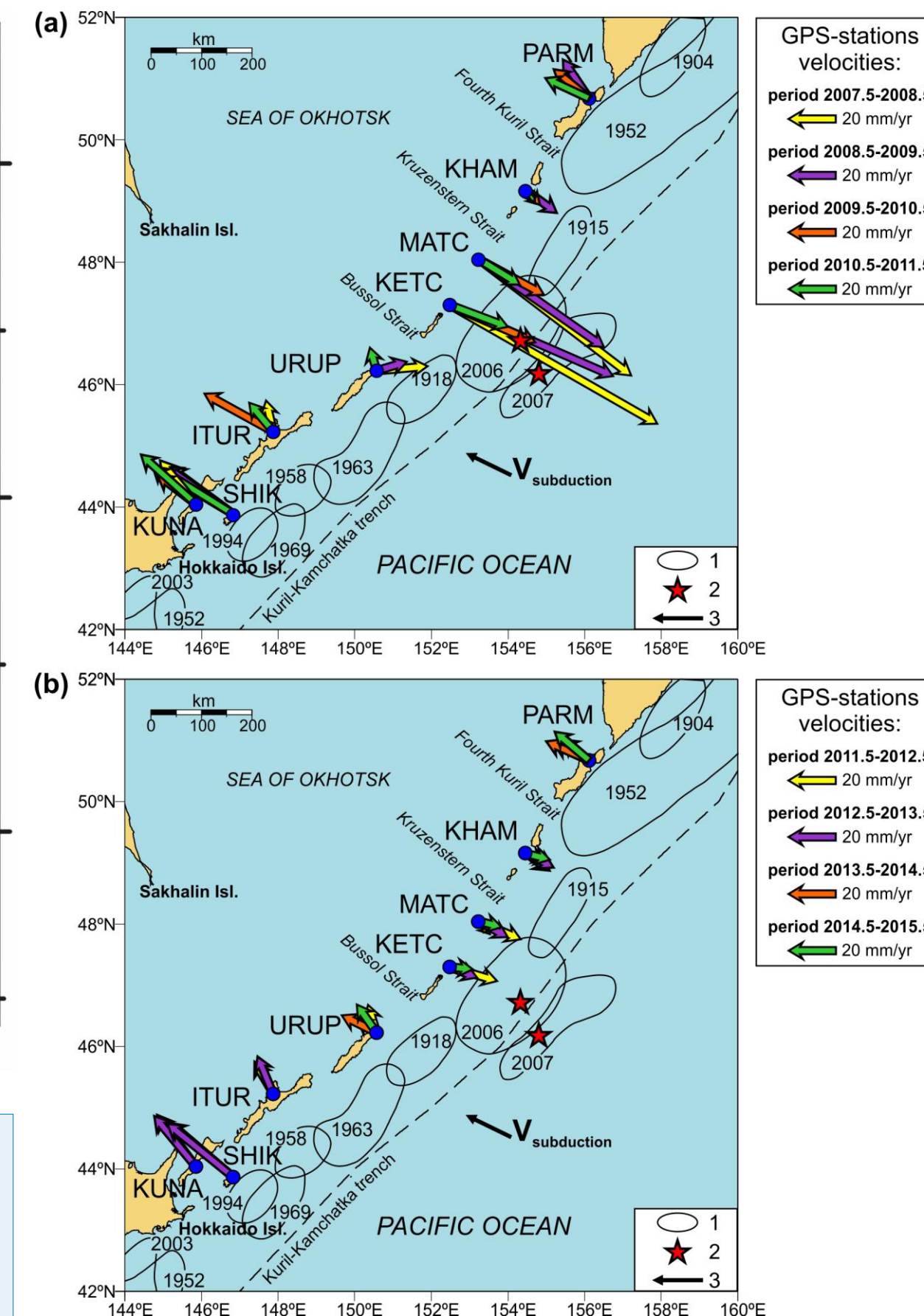


Fig.7 Annual variations of station velocities over the 8-th year period after 2006 Simushir earthquake

We made an inversion of obtained coseismic offsets (Fig. 8) using STATIC1D software [Pollitz, 1996] to construct the models of slip distributions in the sources of Simushir earthquakes (Fig. 9). The obtained models are in good agreement with a similar model constructed earlier on the basis of GNSS data (Fig. 10).

We calculated the seismic moments for our distributions, which were 5.93×10^{21} N·m for the 2006 earthquake and 2.98×10^{21} N·m for the 2007 earthquake. The obtained values are consistent with those obtained in [Steblov et al., 2008] within 15% and are about 1.5 times higher than those provided by GCMT [Ekström et al., 2012]. Overall, the area of maximum coseismic displacement in the source affected three seismogenic blocks from 5 to 7 (Fig. 9).

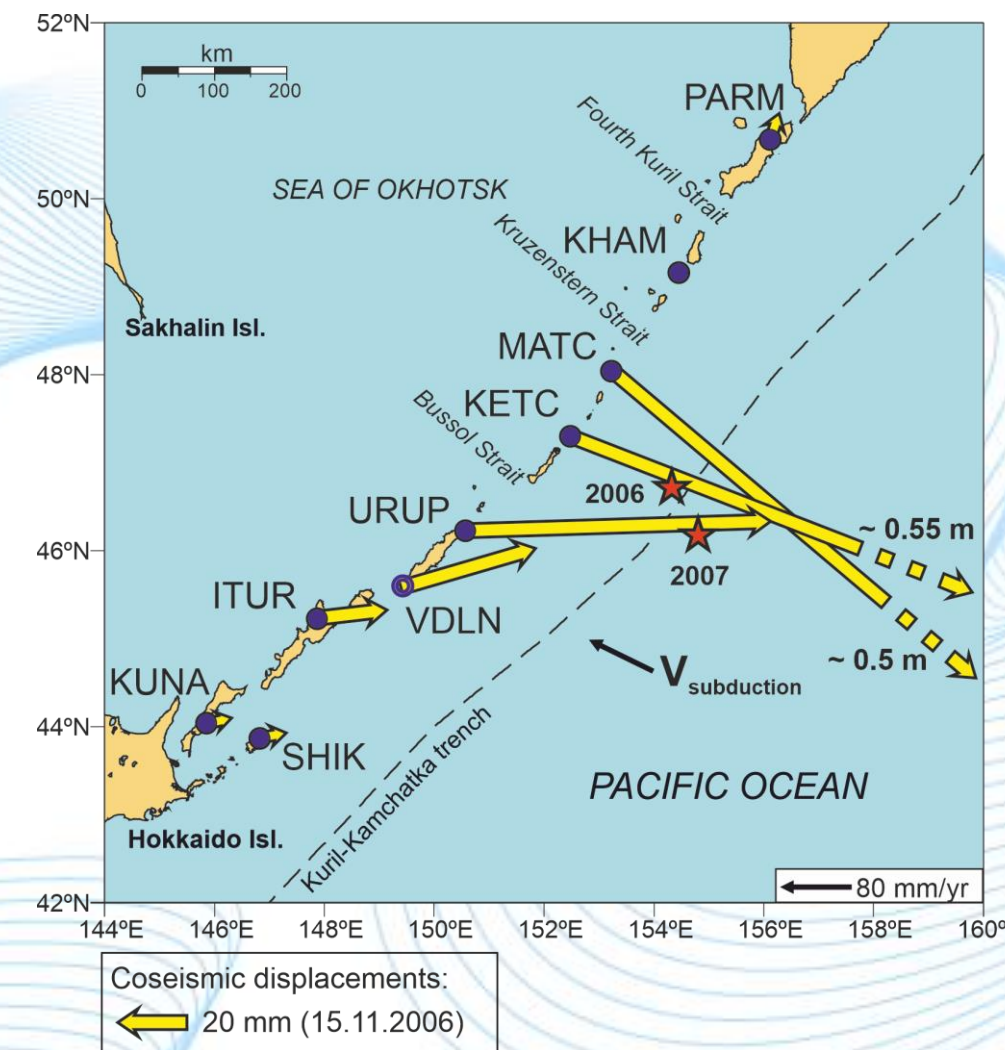


Fig.8 Coseismic offsets during the 2006 Simushir earthquake.

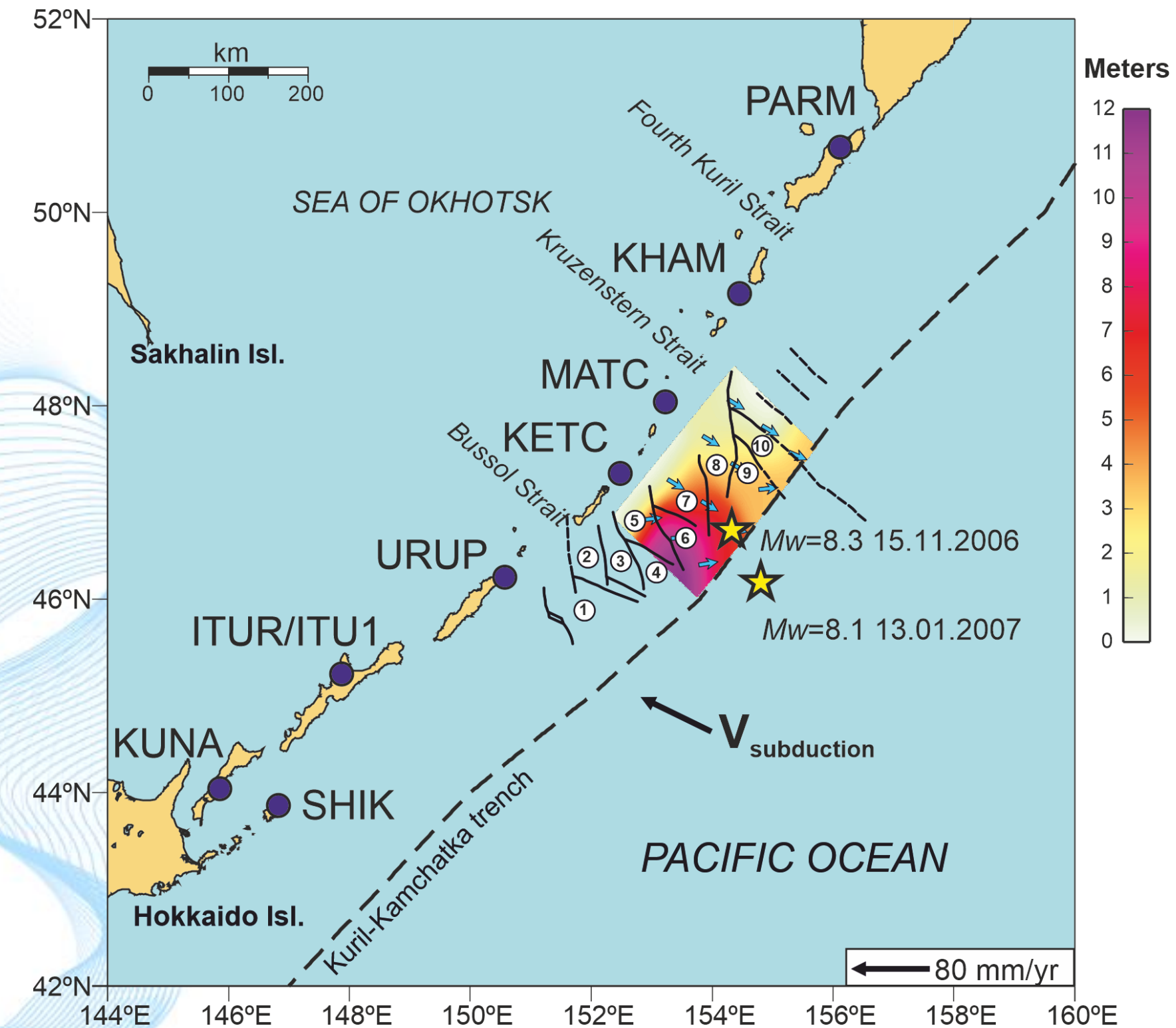


Fig.9 Model of slip distribution in the source of the 2006 Simushir obtained on the basis of coseismic displacements [Vladimirova et al., 2020]. Dashed lines indicate faults that outlined seismogenic blocks [Baranov et al., 2015].

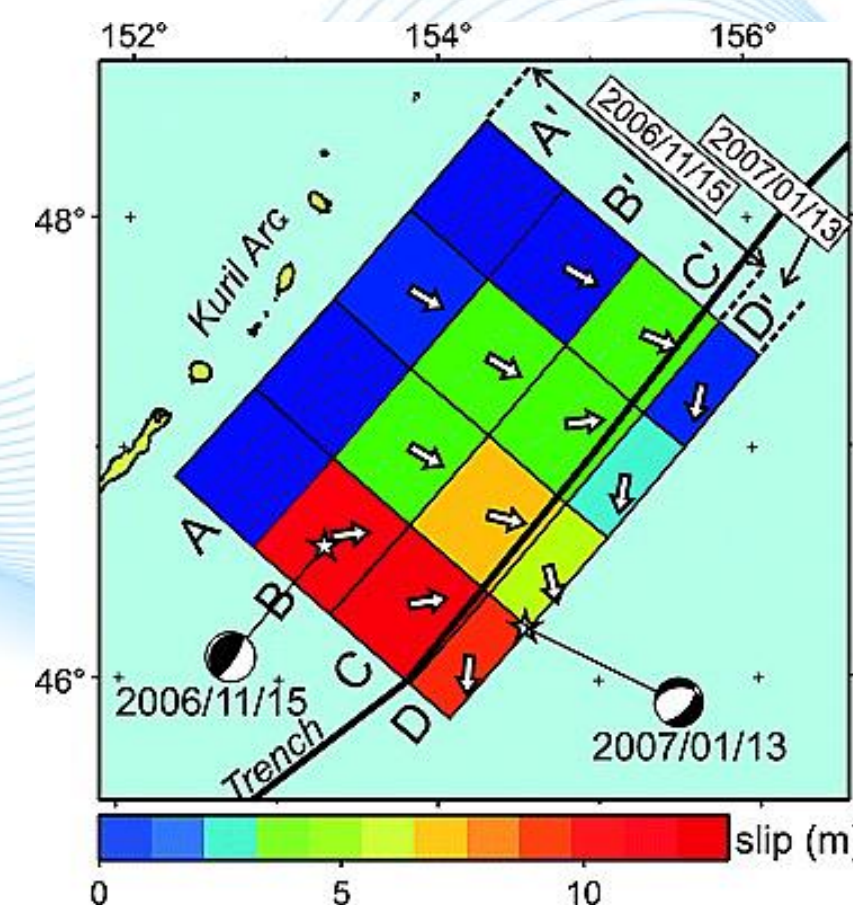


Fig.10 Models of the 2006-2007 Simushir earthquake source from [Steblov et al., 2008]

We assume that in the first months after the 2006 earthquake the predominant postseismic process was afterslip over the fault plane. This consideration can explain the lateral extension of the initial source of the 2006 earthquake, which, in turn, causes recorded postseismic motion of the sites URUP and KHAM. To check this hypothesis we built a qualitative model of afterslip in the source of the 2006 earthquake using two-months postseismic GNSS data, recorded at the sites PARM, URUP, ITUR, KUNA and SHIK. The calculated slip distribution in the source affects adjacent seismogenic blocks but rapidly decreases (Fig. 11). Thus, the constructed afterslip model confirms the lateral extension of the initial rupture of the 2006 earthquake and supports the assumption of the dominance of viscoelastic relaxation from more than six months after the earthquake.

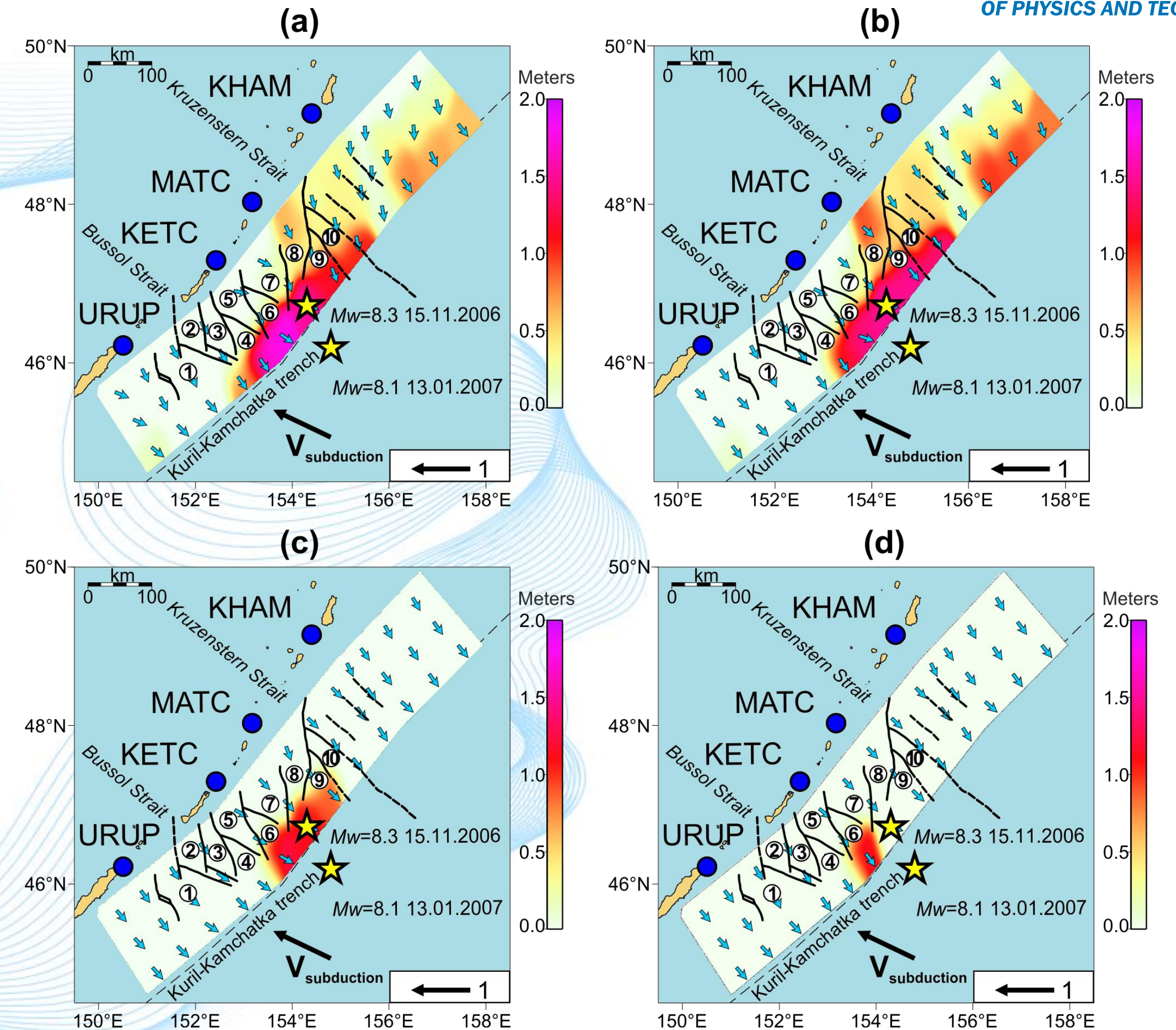


Fig.11 Inversions for afterslip after the 2006 Simushir earthquake [Vladimirova et al., 2020]. Inversions were performed over the two-week intervals: (a) from 16/11/2006 to 30/11/2006; (b) from 01/12/2006 to 15/12/2006; (c) from 16/12/2006 to 30/12/2006; (d) from 31/12/2006 to 12/01/2007.

Our results	Future plans
<ul style="list-style-type: none">• The proposed KurilNet data processing approach combining direct modeling and regression analysis allows us to identify individual components of the station displacements caused by the dynamics of the subduction zone.• Obtained components of displacements were used to model geodynamical processes associated with the 2006-2007 Simushir earthquakes.	<ul style="list-style-type: none">• Implementation of single-station and network-based algorithms for detection of transients.• A more thorough study of the periodic components of the time series using autocorrelation algorithm.

1. Baranov, B.V., Ivanchenko, A.I., & Dozorova, K.A. (2015). The Great 2006 and 2007 Kuril Earthquakes, Forearc Segmentation and Seismic Activity of the Central Kuril Islands Region. *Pure and Applied Geophysics*, 172(12), 3509–3535.
2. Bedford, J., Moreno, M., Li, S., Oncken, O., Baez, J.C., Bevis, M., et al. (2016). Separating rapid relocking, afterslip, and viscoelastic relaxation: Application of the postseismic straightening method to the Maule 2010 cGPS. *Journal of Geophysical Research: Solid Earth*, 121, 7618–7638, <https://doi.org/10.1002/2016JB013093>
3. Ekström, G., Nettles, M., & Dziewonski, A.M. (2012). The global CMT project 2004-2010: Centroid-moment tensors for 13,017 earthquakes. *Physics of the Earth and Planetary Interiors*, 200–201, 1–9. doi:10.1016/j.pepi.2012.04.002.
4. Herring, T.A., King, R.W., Floyd, M.A., & McClusky, S.C. (2018a). GAMIT Reference Manual, Release 10.7. GPS Analysis at MIT, http://www-gpsg.mit.edu/~simon/gtgk/GAMIT_Ref.pdf.
5. Herring, T.A., Floyd, M.A., King, R.W., & McClusky, S.C. (2018b). GLOBK, Global Kalman filter VLBI and GPS analysis program, Release 10.7, http://geoweb.mit.edu/gg/GLOBK_Ref.pdf.
6. Kogan, M.G., Vasilenko, N.F., Frolov, D.I. Freymueller, J.T., Steblov, G.M., Prytkov, A.S., et al. (2013). Rapid postseismic relaxation after the great 2006–2007 Kuril earthquakes from GPS observations in 2007–2011, *Journal of Geophysical Research*, 118, 3691–3706. doi:10.1002/jgrb.50245.
7. Lobkovsky, L.I., Baranov, B.V., Pristavakina, E.I. and Kerchman, V.I (1991) Analysis of seismotectonic processes in subduction zones from the standpoint of a keyboard model of great earthquakes. *Tectonophysics*. V. 199. I. 2–4. P. 211–236.
8. Lobkovsky, L.I., Vladimirova, I.S., Gabsatarov, Y.V., Garagash, I. A., Baranov, B.V., & Steblov, G.M. (2017). Post-seismic motions after the 2006–2007 Simushir earthquakes at different stages of the seismic cycle. *Doklady Earth Sciences*, 473(1), 375–379.
9. Pollitz, F.F. (1996). Coseismic deformation from earthquake faulting on a layered spherical earth. *Geophysical Journal International*, 125 (1), 1–14. doi:10.1111/j.1365-246X.1996.tb06530.x.
10. Pollitz, F.F. (1997). Gravitational viscoelastic postseismic relaxation on a layered spherical earth. *Journal of Geophysical Research*, 102, 17921–17941.
11. Steblov, G.M., Kogan, M.G., Levin, B.V., Vasilenko, N.F., Prytkov, A.S., & Frolov, D.I. (2008). Spatially linked asperities of the 2006–2007 great Kuril earthquakes revealed by GPS. *Geophysical Research Letters*, 35, L22306. doi:10.1029/2008GL035572.
12. Vladimirova, I.S., Lobkovsky, L.I., Gabsatarov, Y.V., Steblov, G.M., Vasilenko, N.F., Frolov, D.I., Prytkov, A.S. (2020). Patterns of seismic cycle in the Kuril Island arc from GPS observations. *Pure and Applied Geophysics*. (in press, doi:10.1007/s00024-020-02495z).